Snap-Through Truss as a Vibration Absorber

K. V. AVRAMOV
Department of Theoretical Mechanics, National Technical University "KPI", Frunze Street 21, Kharkov 61002, Ukraine

YU. V. MIKHLIN
Department of Applied Mathematics, National Technical University "KPI", Frunze Street 21, Kharkov 61002, Ukraine

(Received 31 October 2002; accepted 22 April 2003)

Abstract: In this paper we consider the possibility of elastic oscillation absorption using the snap-through truss. This truss was introduced by Mises in 1923. A single-degree-of-freedom linear oscillator is chosen as the most simple model of a continuous elastic system. The nonlinear absorber with three equilibrium positions (the snap-through truss) is attached to this oscillator. The dynamics of this system is studied by the nonlinear normal vibration mode approach. The construction and stability analysis of the localized and non-localized nonlinear normal modes are developed. If the localized mode is realized, the system energy is concentrated in the nonlinear absorber. This situation is the most appropriate to absorb vibrations.

Key Words: Vibration absorber, snap-through truss, stability of nonlinear normal modes

1. INTRODUCTION AND PROBLEM FORMULATION

Numerous scientific publications contain a description and analysis of different devices for the vibration absorption of machines and mechanisms. Here, only some of these publications are selected, those which are related to passive absorbers. In particular, Haxton and Barr (1972) considered the absorber in the form of a beam, which is attached to the system mass–spring. Shaw and Wiggins (1988) considered a pendulum-type centrifugal vibration absorber of torsion oscillations. They used the Melnikov function to study chaotic motions. Shaw et al. (1989) showed analytically that the unstable oscillations appeared, if forced frequency was close to the half-sum of two natural frequencies. In this case, the steady motions were almost periodic. Natsiavas (1992) proposed the use of the oscillator with a nonlinear spring to absorb forced oscillations of the Duffing system. Natsiavas (1993) used the mass–spring nonlinear system to reduce vibrations of the self-excited system. He studied the dynamics using perturbation methods. The general theory of linear and nonlinear absorbers is presented in Frolov (1995). Lee and Shaw (1995) considered the absorption of torsion vibrations of a four-stroke, four-cylinder engine by means of the pendulum-type centrifugal absorber. Haddow and Shaw (2001) studied experimentally the rotating machinery with the centrifugal pendulum absorber. Note that such absorbers are used in the engines of aircrafts

Journal of Vibration and Control, **10:** 291–308, 2004 DOI: 10.1177/1077546304035604

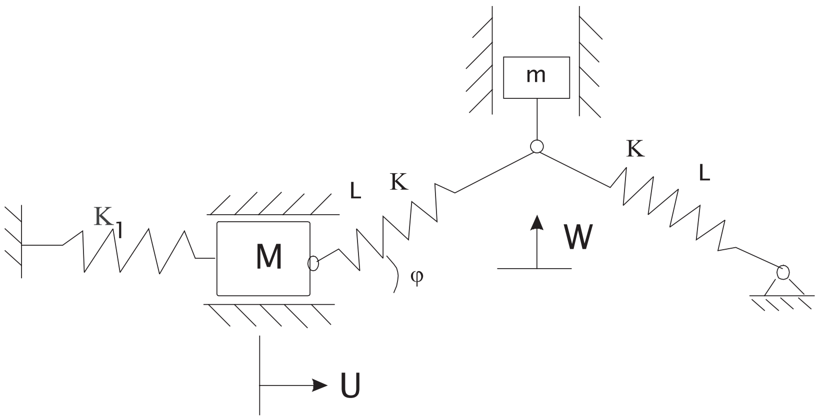

Figure 1. The model under consideration.

and automobiles. Vakakis (2001) considered a semi-infinite linear chain with an essentially nonlinear spring, which was attached to the chain to absorb the energy of oscillations.

Impact systems can be used to absorb oscillations (Karyeaclis and Caughey, 1989a, 1989b). Later Aoki and Watanabe (1994) offered the impact absorber, which contained small mass hitting on the stop. The inverted pendulum with motion limiting stops was used as a vibration absorber by Shaw and Shaw (1989).

Note that the snap-through truss was used in vibration insulation systems with quasi-zero stiffness (Alabuchev et al., 1986). However, this is another application of the snap-through truss in comparison with the absorber considered here.

In this paper, we suggest using a snap-through truss for longitudinal oscillation absorption of an elastic solid. In this case, part of the elastic oscillation energy is transferred to the truss, which jumps from one equilibrium position to another. An elastic system is approximated by the single-degree-of-freedom (1-DOF) mass–spring model to study the truss capacity to absorb oscillations. Free oscillations of 2-DOF systems are studied in this paper using the method of the nonlinear normal modes (NNMs) of vibrations (Vakakis et al., 1996; Manevitch et al., 1989). Note that, if oscillations with large amplitudes are analyzed, this NNM approach is particularly effective. In the case of the appropriate mode for an absorption, the main elastic system and absorber have small and significant amplitudes, respectively. We stress that this motion corresponds to the localized NNM (Vakakis et al., 1996). By assumption, the truss is shallow and its mass and stiffness are significantly smaller then the corresponding parameters of the main elastic system. Such a choice of parameters is determined by the real absorber design conditions.

2. EQUATIONS OF MOTIONS

Figure 1 shows the system under consideration. In this paper we investigate the principle capacity of the small mass snap-through truss to absorb vibrations. Therefore, the 1-DOF main elastic system is considered to simplify the analysis.

This problem has engineering applications. For example, the considered model corresponds to the problem of beam longitudinal vibration absorption. In this paper we show that large amplitude vibrations of the 1-DOF snap-through truss are able to absorb the energy of the linear elastic system vibrations. We stress that if the problem of absorption is solved, the small damping only improves this solution.

The equations of motions are

$$M\ddot{U} + \kappa_1 U + \kappa \left[U - L\cos\varphi + L\left\{ 1 + \frac{W^2}{(L\cos\varphi - U)^2} \right\}^{-1/2} \right] = 0;$$
$$m\ddot{W} + \kappa W \left[2 - L\left\{ (L\cos\varphi - U)^2 + W^2 \right\}^{-1/2} - L\left\{ L^2\cos^2\varphi + W^2 \right\}^{-1/2} \right] = 0, \tag{1}$$

where (U, W) are the generalized coordinates, L is the length of the spring, φ is the angle, which is defined the equilibrium position, κ is the spring stiffness of the truss, and κ_1 is the stiffness of the main elastic system. The system (1) has three equilibrium positions: one saddle, $(U, W) = \left(\dfrac{\kappa L(\cos\varphi - 1)}{\kappa_1 + \kappa}; 0 \right)$ and two centers $(U, W) = (0; \pm L\sin\varphi)$.

The dimensionless variables $u = \dfrac{U}{L}$; $w = \dfrac{W}{L}$ and dimensionless time: $t = \sqrt{\dfrac{M}{\kappa_1}}\tau$ are introduced. Then the system (1) takes the following form:

$$\ddot{u} + u + \gamma \left[u - \cos\varphi + \left\{ 1 + \frac{w^2}{(\cos\varphi - u)^2} \right\}^{-1/2} \right] = 0;$$
$$\mu\ddot{w} + \gamma w \left[2 - \left\{ (\cos\varphi - u)^2 + w^2 \right\}^{-1/2} - \left\{ \cos^2\varphi + w^2 \right\}^{-1/2} \right] = 0; \tag{2}$$
$$\gamma = \frac{\kappa}{\kappa_1};\ \mu = \frac{m}{M}.$$

The new variable is introduced: $u_1 = u + \dfrac{\gamma(1-\kappa)}{1+\gamma}$. If the oscillation absorption takes place, then the stable localized vibration mode exists, and $u_1 << w$. With the assumption of Section 1, the mass and stiffness of the truss are significantly smaller than the corresponding parameters of the elastic system. Therefore, the following relations are introduced: $\mu = \varepsilon\bar{\mu}$; $\gamma = \varepsilon\bar{\gamma}$; $\varepsilon \prec\prec 1$. Retaining linear, quadratic and cubic terms by u_1 and w we can rewrite the system (2) as

$$\ddot{u}_1 + (1 + \varepsilon\bar{\gamma})u_1 - \frac{\varepsilon\bar{\gamma}}{\rho^3}u_1 w^2 - \frac{\varepsilon\bar{\gamma}}{2\rho^2}w^2 = 0; \tag{3}$$

$$\bar{\mu}\ddot{w} - \bar{\gamma}\alpha^2 w - \frac{\bar{\gamma}}{\rho^2}wu_1 + \frac{\bar{\gamma}\beta^2}{2}w^3 = 0, \tag{4}$$

where $$\rho = \frac{\gamma + \kappa}{1+\gamma};\ \alpha^2 = \frac{1}{\rho} + \frac{1}{\kappa} - 2;\ \beta^2 = \frac{1}{\rho^3} + \frac{1}{\kappa^3}. \tag{5}$$

3. PERIODIC MOTION ANALYSIS

3.1. Periodic Motions with Small Amplitudes

Let us consider the oscillations close to the stable equilibrium of the snap-through truss: $w = \sin\varphi;\ u = 0$. We use the following change of variables: $w - \sin\varphi = \varepsilon w_1;\ u_1 = \varepsilon u_2$. Substituting the latter formulae into the system (3) and (4) and taking into account the relations (5), we can obtain after some transformations the following system

$$\ddot{u}_2 + (1 + \varepsilon\bar{\gamma}c^2)u_2 - \varepsilon\bar{\gamma}csw_1 + \varepsilon^2\bar{\gamma}\left[\tilde{\beta}\, w_1u_2 + \tilde{\alpha}\, w_1^2 - \frac{3}{2}s^2cu_2^2\right] = 0;$$
$$\bar{\mu}\,\ddot{w}_1 + \bar{\gamma}\,(2s^2w_1 - scu_2) + \varepsilon\bar{\gamma}\left\{3sc^2w_1^2 + \frac{\tilde{\beta}}{2}u_2^2 + 2\tilde{\alpha}\, w_1u_2\right\} = 0; \tag{6}$$

where $\tilde{\beta} = s - 3sc^2;\ \tilde{\alpha} = \frac{3}{2}s^2c - \frac{c}{2};$ here $s = \sin\varphi;\ c = \cos\varphi$.

For $\varepsilon = 0$ the linear system (6) permits two NNM modes, which are changed at $\varepsilon \neq 0$. System (6) is rewritten to analyze such NNMs in the following form

$$\ddot{u}_2 + \tilde{\prod}{}'_{u_2} = 0;\ \varepsilon\bar{\mu}\,\ddot{w}_1 + \tilde{\prod}{}'_{w_1} = 0; \tag{7}$$

$$\tilde{\prod} = (1 + \varepsilon\bar{\gamma}c^2)\frac{u_2^2}{2} + \varepsilon\bar{\gamma}s^2w_1^2 - \varepsilon\bar{\gamma}csw_1u_2 + \varepsilon^2\bar{\gamma}\left\{\frac{\tilde{\beta}}{2}w_1u_2^2 + \tilde{\alpha}\, w_1^2u_2 + sc^2w_1^3 - \frac{s^2c}{2}u_2^3\right\},$$

where $\tilde{\prod}$ is the system potential energy, and $\tilde{\prod}{}'_{u_2};\ \tilde{\prod}{}'_{w_1}$ are derivatives with respect to u_2 and w_1. Following the NNM approach (Vakakis et al., 1996), trajectories of the modes in system (7) configuration space are sought in the form: $u_2 = u_2(w_1)$. We use the following equations to eliminate t from equations (7):

$$\frac{\mathrm{d}(\circ)}{\mathrm{d}t} = \dot{w}_1\frac{\mathrm{d}(\circ)}{\mathrm{d}w_1};\ \frac{\mathrm{d}^2(\circ)}{\mathrm{d}t^2} = \dot{w}_1^2\frac{\mathrm{d}^2(\circ)}{\mathrm{d}w_1^2} + \ddot{w}_1\frac{\mathrm{d}(\circ)}{\mathrm{d}w_1}. \tag{8}$$

Using relations (8) and the system (7) energy integral

$$\frac{\dot{u}_2^2}{2} + \varepsilon\bar{\mu}\,\frac{\dot{w}_1^2}{2} + \tilde{\prod} = h, \tag{9}$$

we derive the following equation to obtain the trajectories:

$$\frac{2\left(h - \tilde{\prod}\right)}{u_2'^2 + \varepsilon\bar{\mu}}u_2'' - \frac{\tilde{\prod}{}'_{w_1}}{\varepsilon\bar{\mu}}u_2' = -\tilde{\prod}{}'_{u_2}. \tag{10}$$

Note that h is the total system energy. Equation (10) has the singularity at the maximum isoenergetic surface $\tilde{\prod} = h$. Therefore, equation (10) is supplemented by the boundary conditions

$$\left.\left(\frac{\tilde{\prod}'_{w_1}}{\varepsilon\bar{\mu}}u'_2 - \tilde{\prod}'_{u_2}\right)\right|_{\tilde{\prod}=h} = 0,$$

which are the conditions of orthogonality of the NNMs to the maximum isoenergetic surface. These conditions provide the NNM trajectories analytical continuation on surface $\tilde{\prod} = h$.

3.1.1. Localized Periodic Motions $u_2 = \varepsilon\bar{u}_2\,(w_1)$

The small oscillations of system (7) are presented in the form $u_2 = \varepsilon\bar{u}_2\,(w_1)$, then the equation (10) first approximation with respect to ε has the form:

$$\left(\bar{h} - \bar{\gamma}s^2w_1^2\right)\bar{u}''_2 - \bar{\gamma}s^2w_1\bar{u}'_2 - \left(\bar{\gamma}csw_1 - \bar{u}_2\right)\frac{\bar{\mu}}{2} = 0; \tag{11}$$
$$h = \varepsilon\bar{h}.$$

Let us present the equation (11) solutions as the power series:

$$\bar{u}_2 = b_0 + b_1w_1 + b_2w_1^2 + \ldots \tag{12}$$

Using energy integral (9), oscillations amplitudes $W_*^{(\max)}$ are determined on surface $\tilde{\prod} = h$:

$$W_*^{(\max)} = \sqrt{\frac{\bar{h}}{\bar{\gamma}s^2}}. \tag{13}$$

The first approximation with respect to ε of the boundary conditions has the form:

$$\left.\left\{\bar{\gamma}s^2w_1\bar{u}'_2 + (\bar{\gamma}csw_1 - \bar{u}_2)\frac{\bar{\mu}}{2}\right\}\right|_{w_1=\pm W_*^{(\max)}} = 0. \tag{14}$$

Series (12) is substituted into equation (11) and we match respective powers of w_1. Let us restrict ourselves to powers w_1^0, w_1, w_1^2. Then we obtain three linear algebraic equations with respect to five unknowns $b_0, \ldots, b_4$. Satisfying boundary conditions (14), two additional linear algebraic equations are derived. The solution of the system of five algebraic equations is

$$b_1 = \frac{\bar{\gamma}cs}{1 - 2p^2s^2}; \quad b_0 = b_2 = b_3 = b_4 = 0, \tag{15}$$

where $p^2 = \dfrac{\bar{\gamma}}{\bar{\mu}}$.

As a result, the localized NNM has been derived: $u_2 = \varepsilon b_1w + O\,(\varepsilon^2)$. Thus the obtained trajectory in configuration space $(w_1, u_2) \in R^2$ is a straight line close to the y-axis. The analytical solution accuracy is illustrated by the Runge–Kutta method calculations of system (3) and (4) with the following parameters: $\varphi = 0.15$; $\mu = \gamma = \varepsilon = 0.01$. The initial conditions are chosen from the analytical results, i.e. $\dot{u}_2(0) = \dot{w}(0) = 0$; $w(0) = W_*^{(\max)}$; $u_2(0) = \varepsilon b_1W_*^{(\max)}$. Figure 2 shows the very good agreement between the analytical solution and the numerical calculations, which are presented in the configuration space.

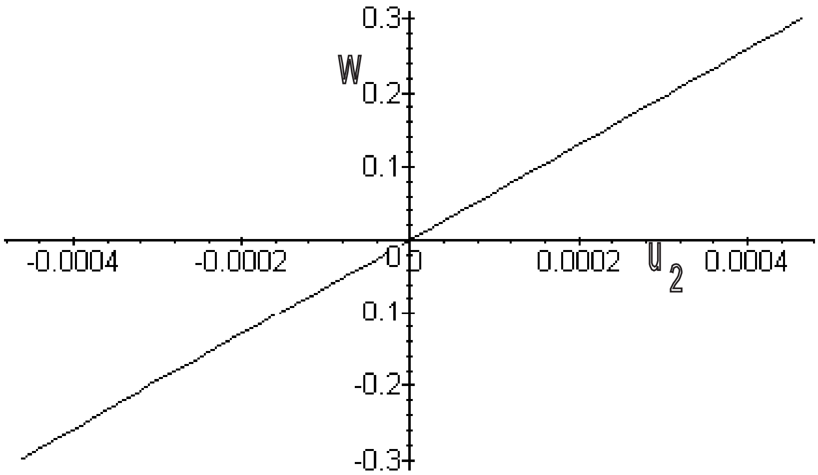

Figure 2. The localized NNM with small amplitudes. Comparison of the analytical and numerical solutions.

3.1.2. Non-Localized Periodic Motions $u_2 = gw_1 + \varepsilon u_3(w_1)$

The second non-localized NNM of vibrations has the following form:

$$u_2 = gw_1 + \varepsilon u_3(w_1). \tag{16}$$

Equation (10) for motions (16) can be written in the form:

$$\varepsilon 2u_3'' \left(\frac{h}{g^2} - \frac{w_1^2}{2} \right) - p^2 \left[g\left(2s^2 - csg\right) w_1 + \varepsilon \left\{ g\left(Bw_1^2 - csu_3\right) + u_3' w_1 \left(2s^2 - csg\right) \right\} \right] + \tilde{\prod}'_{u_3} = 0;$$

$$B = \frac{1}{2}\tilde{\beta}\, g^2 + 2\tilde{\alpha}\, g + 3sc^2. \tag{17}$$

Two approximations of the solutions with respect to ε are obtained by matching the respective powers of ε. As a result, we derive two ordinary differential equations. Value g is obtained from the first of these:

$$g = \frac{1}{sc}\left(2s^2 - p^{-2}\right). \tag{18}$$

The second equation is

$$2u_3'' \left(\frac{h}{g^2} - \frac{w_1^2}{2} \right) - p^2 \left\{ g\left(Bw_1^2 - csu_3\right) + u_3' w_1 \left(2s^2 - csg\right) \right\} + u_3 + \bar{\gamma} c^2 g w_1 - \bar{\gamma} c s w_1 = 0. \tag{19}$$

The solutions of equation (19) can be presented in the form of the power series:

$$u_3 = c_0 + c_1 w_1 + c_2 w_1^2 + \dots \tag{20}$$

Oscillation amplitude $W_1^{(\max)}$ is derived from the energy integral $\tilde{\prod}\left(W_1^{(\max)}\right) = h$ when the kinetic energy is equal to zero. Then parameter $W_1^{(\max)}$ is determined in the following way:

$$W_1^{(\max)} = \sqrt{\frac{2h}{g^2}}. \tag{21}$$

Two boundary conditions on the surface $\tilde{\prod}\left(W_1^{(\max)}\right) = h$ are

$$\left\{-p^2\left[g\left(Bw_1^2 - csu_3\right) + u_3' w_1\left(2s^2 - csg\right)\right] + u_3 + \bar{\gamma}c^2 g w_1 - \bar{\gamma} csw_1\right\}\Big|_{w_1 = \pm W_1^{(\max)}} = 0. \tag{22}$$

Substituting series (20) into equations (19) and (22), the linear algebraic equation system with respect to the coefficients of series (20) is obtained. The solution of this algebraic system can be written as

$$c_0 = -\frac{hB}{gs^2\left(s^2p^2 - 2\right)}; \quad c_1 = \bar{\mu}\left(\frac{1}{g} - \frac{c}{s}\right); \quad c_2 = \frac{p^2 gB}{2\left(s^2p^2 - 2\right)}; \quad c_3 = c_4 = 0. \tag{23}$$

Thus the second NNM has been derived in the form (20).

System (3) and (4) is integrated numerically to check the analytical results with the system parameters chosen in Section 3.1.1 and initial conditions corresponding to the NNM (20):

$$u_2(0) = kW_1^{(\max)} + \varepsilon u_3\left(W_1^{(\max)}\right); \quad w_1(0) = W_1^{(\max)}; \quad \dot{u}_1(0) = \dot{w}_1(0) = 0.$$

Figure 3 shows the numerical simulation results in the configuration space.

3.2. Localized Periodic Motions with Large Amplitudes

Here periodic motions of system (3) and (4) with large amplitudes are also studied by using the NNM approach. Then system (3) and (4) can be written in the following form

$$\ddot{u}_1 + \frac{\partial \prod}{\partial u_1} = 0; \quad \mu\ddot{w} + \frac{\partial \prod}{\partial w} = 0; \tag{24}$$

$$\prod = (1 + \varepsilon\bar{\gamma})\frac{u_1^2}{2} - \frac{\varepsilon\bar{\gamma}u_1^2}{2\rho^3} - \frac{\varepsilon\bar{\gamma}w^2 u_1}{2\rho^2} - \frac{\varepsilon\bar{\gamma}\alpha^2 w^2}{2} + \frac{\varepsilon\bar{\gamma}\beta^2 w^4}{8},$$

where $\prod$ is the system potential energy. Let us determine the system (24) periodic motions in the form $u_1 = u_1(w)$. The equation of trajectories in the configuration space has the following form:

$$u_1''(w)\frac{2\left(h - \prod\right)}{u_1'^2 + \mu} - \frac{1}{\mu}\prod\nolimits_w' u_1' = -\prod\nolimits_{u_1}'. \tag{25}$$

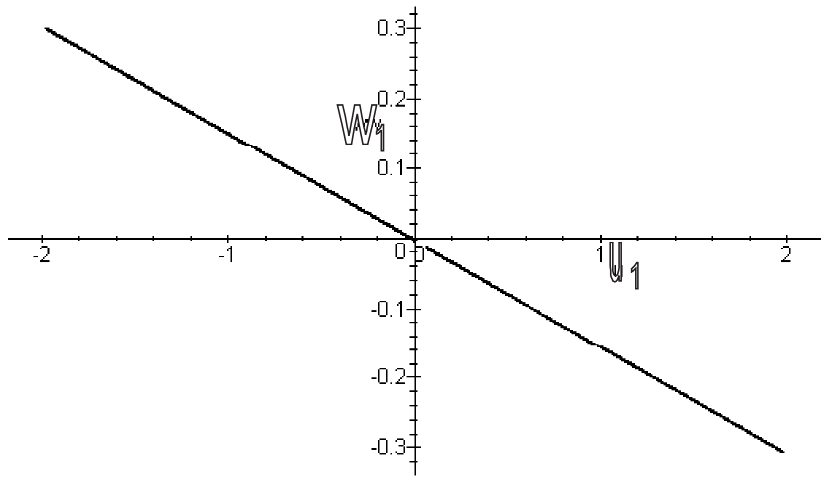

Figure 3. The non-localized NNM with small amplitudes. Comparison of the analytical and numerical solutions.

The solution of equation (25) is presented as

$$u_1 = \varepsilon \bar{u}_1(w); \quad \bar{u}_1(w) = a_0 + a_1 w + a_2 w^2 + \dots \tag{26}$$

where $a_0, a_1, \dots$ are unknown coefficients. Series (26) is substituted into equation (25) and matching of respective powers of w is carried out. Restricting ourselves to orders w^0, w^1, w^2, three linear algebraic equations with respect to five variables $a_0, \dots, a_4$ are derived. Two boundary conditions at the maximal equipotential surface $\prod = h$ give us two additional algebraic equations

$$\left\{ \frac{1}{\mu} \prod\nolimits_w' u_1' - \prod\nolimits_{u_1}' \right\} \Bigg|_{w=\pm W_*}, \tag{27}$$

where W_* is an amplitude of the NNM. The equation for W_* determination is obtained from the energy integral when a kinetic energy $T = 0$. This equation is

$$\prod \Big|_{w=\pm W_*} = h. \tag{28}$$

The previous equation can be written in the form

$$\bar{h} = \frac{\bar{\gamma}\beta^2}{8} W_*^4 - \frac{\bar{\gamma}\alpha^2}{2} W_*^2; \quad h = \varepsilon \bar{h}. \tag{29}$$

We derive two equations from boundary conditions (27). We add these equations to the previously obtained three linear algebraic equations. Solving the system of five linear algebraic equations with respect to $a_0, \dots, a_4$, we derive the outcome:

$$a_1 = a_3 = 0; \quad a_0 = -\frac{4\bar{h}}{\bar{\mu}} a_2;$$

$$\tilde{a}_2 = \left\{ \left(2 - \frac{(\bar{\mu} + 4\bar{\gamma}\alpha^2) W_*^2}{12\bar{h}} \right) \left(4\bar{\gamma}\alpha^2 - 2\bar{\gamma}\beta^2 W_*^2 + \bar{\mu} \right) + \bar{\gamma}\beta^2 W_*^2 \right\}^{-1}$$
$$\times \left\{ 2\bar{\mu} - \frac{\bar{\mu} W_*^2}{12\bar{h}} \left(4\bar{\gamma}\alpha^2 - 2\bar{\gamma}\beta^2 W_*^2 + \bar{\mu} \right) \right\}; \tag{30}$$
$$\tilde{a}_4 = \frac{\bar{\mu}}{24\bar{h}} - \frac{\bar{\mu} + 4\bar{\gamma}\alpha^2}{24\bar{h}} \tilde{a}_2; \quad a_j = \tilde{a}_j \frac{\bar{\gamma}}{2\rho^2}; \quad j = 2, 4.$$

So, the NNM trajectory of the essentially nonlinear system is obtained in the form (26) and (30).

The following values of the parameters are taken for the numerical calculations: $\mu = \gamma = \varepsilon = 0.01$; $\varphi = 0.15$. The next initial conditions correspond to the analytical solution (26) and (30): $u_2(0) = \varepsilon \bar{u}_2 (W_*)$; $w(0) = W_*$; $\dot{u}_2(0) = \dot{w}(0) = 0$.

Figure 4(a) shows the NNM of vibrations, which is obtained according to formulae (26) and (30). Figure 4(b) shows the corresponding numerical results.

As we can see from Figure 4, the snap-through truss has significant amplitudes of oscillations and the main elastic system has small amplitudes. If such motions are stable, this guarantees the vibration absorption. Thus, the stability analysis of the obtained solutions can answer finally the question about the possible vibration absorption.

4. PERIODIC MOTION STABILITY

In this section we use a small curvature of the obtained NNMs to analyze their stability. The rectilinear approximations of these trajectories are restricted to the analysis. Let us introduce new variables (ξ, η) in the following way. The ξ-axis is directed along the rectilinear approximation of the NNM trajectory and the η-axis has the orthogonal direction. Figure 5 shows these axes and the qualitative behavior of solutions close to some unstable NNM. Orthogonal variation $\eta(t)$ defines the orbital stability of NNMs. Therefore, the problem is reduced to the analysis of a single linear differential equation.

4.1. Stability of the Periodic Motions with Large Amplitudes

Let us consider the stability of periodic motions, which were determined in the Section 3.2. It is possible to rewrite system (3) and (4) taking into account that $u_1 = O(\varepsilon)$ (see relations (26)) and introducing the following representation: $w = w_0 + O(\varepsilon)$. Retaining the lowest-order terms in ε we have the following equations:

$$\ddot{w}_0 - p^2\alpha^2 w_0 + \frac{p^2\beta^2}{2} w_0^3 = 0;$$
$$\ddot{u}_1 + (1 + \varepsilon\bar{\gamma}) u_1 - \frac{\varepsilon\bar{\gamma} u_1 w_0^2}{\rho^3} - \frac{\varepsilon\bar{\gamma} w_0^2}{2\rho^2} = 0. \tag{31}$$

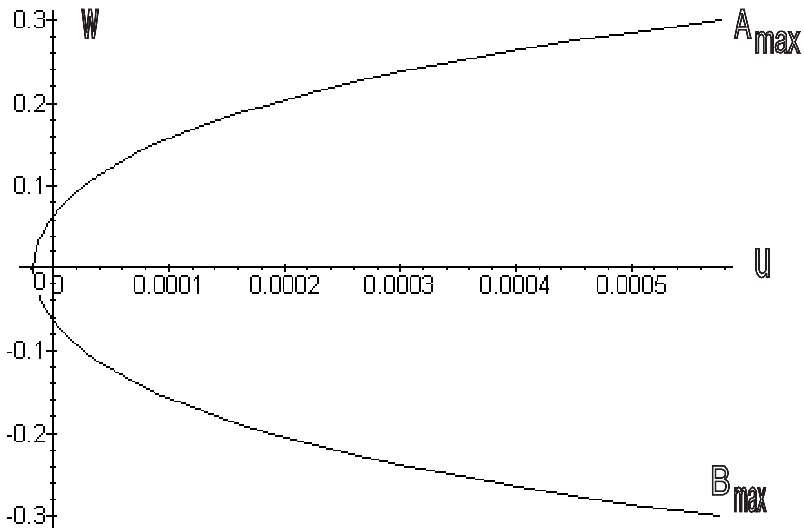

a)

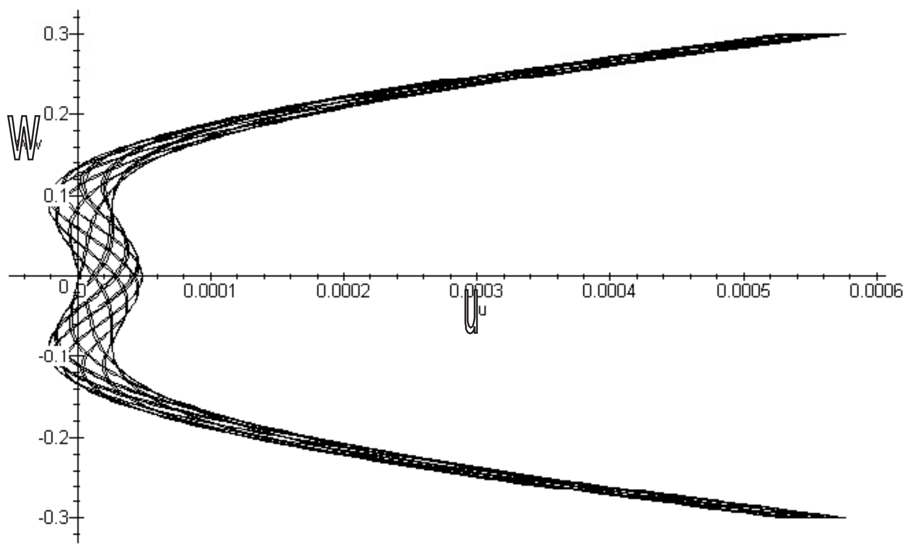

b)

Figure 4. Periodic motion with large amplitude: (a) analytical solution; (b) numerical simulation with initial conditions, which correspond to the analytical results.

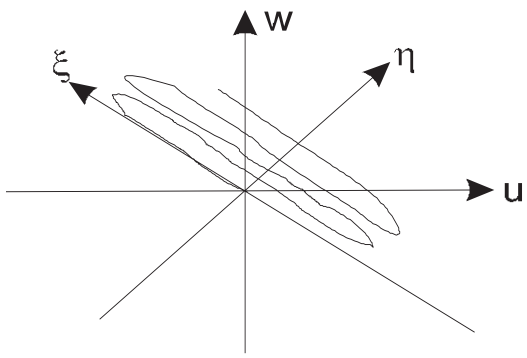

Figure 5. Qualitative behavior of solutions close to some unstable NNM.

Note that the first equation of system (31) is u_1-independent. Let us study small perturbations $\eta(t)$ of periodic motions $\bar{u}_1$, determined by formula (26): $u_1 = \bar{u}_1 + \eta$. As a result, the following differential equation is obtained from the second equation (31)

$$\ddot{\eta} + \left(1 + \varepsilon\bar{\gamma} - \frac{\varepsilon\bar{\gamma}}{\rho^3} w_0^2\right)\eta = 0, \tag{32}$$

where

$$w_0 = \sqrt{2}\frac{\alpha}{\beta}\sqrt{1+\sqrt{1+4H}}\,\mathrm{cn}\left(p\alpha\tau\sqrt[4]{1+4H}; k\right); \tag{33}$$

$$4H = \frac{\beta^4 W_*^4}{4\alpha^4} - \frac{\beta^2}{\alpha^2}W_*^2; \tag{34}$$

$$2k^2 = \left(1 + \frac{\beta^4 W_*^4}{4\alpha^4} - \frac{\beta^2}{\alpha^2}W_*^2\right)^{-1/2} + 1. \tag{35}$$

Note that formula (29) defines a value W_*. The following notations are taken in relations (32)–(35): k is a modulus of elliptic integral; $\mathrm{cn}()$ is an elliptic function; H is a total energy of the oscillator which is determined by the first equation of system (31). Figure 6 shows the phase plane trajectories of this oscillator. Trajectory L represents the vibration absorption, since the snap-through truss has large oscillation amplitudes and the linear elastic system has small amplitudes. Such motions of the snap-through truss are described by formula (33). We derive from equation (35)

$$k^2 = k_0^2 - \varepsilon k_1 + O\left(\varepsilon^2\right); \tag{36}$$

$$k_1 = \frac{\bar{\gamma}\left(1.5 - c^{-1}\right)\left[W_*^4 - 2c^2(1-c)W_*^2\right]c^2(1-c)}{\left[4c^4(1-c)^2 + W_*^4 - 4c^2(1-c)W_*^2\right]^{3/2}};$$

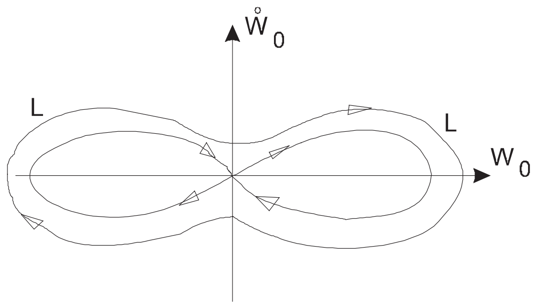

Figure 6. Phase trajectories of the oscillator which is determined by the first equation of system (31).

$$k_0^2 \;=\; 0.5 + \frac{c^2\,(1-c)}{\sqrt{4c^4\,(1-c)^2 + W_*^4 - 4c^2\,(1-c)\,W_*^2}}.$$

Substituting the Fourier series expansion of $\mathrm{cn}^2(t, k_0)$ into equation (32), we can obtain the next equation

$$\ddot{\eta} + \left[\Omega_0^2 - \varepsilon h \sum_{s=1}^{\infty} \frac{s q_0^s}{(1-q_0^{2s})} \cos\left(\Omega_* s t\right)\right] \eta \;=0; \qquad (37)$$

$$h = \bar{\mu}\,\frac{4\pi^2}{K^2\,(k_0)}; \Omega_* = \frac{\pi}{K\,(k_0)}; q_0 = \exp\left[-\frac{\pi K'\,(k_0)}{K\,(k_0)}\right];$$

$$\Omega_0^2 = \frac{c\,(2k_0^2-1)}{2\,(1-c)\,p^2} - \frac{\varepsilon k_1 c}{(1-c)\,p^2} + \frac{\varepsilon \bar{\mu}\,(2k_0^2-1)\,(1+2c)}{4\,(1-c)} - \varepsilon 2\bar{\mu}\left[\frac{E\,(k_0)}{K\,(k_0)} - 1 + k_0^2\right],$$

where $K(k_0)$ and $E(k_0)$ are the complete elliptic integrals of the first and the second kinds.

Equation (37) is analyzed by the multiple scales method (Nayfeh, 1973). The solution of this equation is chosen in the form:

$$\eta \;= \eta_0\,(T_0, T_1) + \varepsilon \eta_1\,(T_0, T_1) + \ldots; T_0 = t; T_1 = \varepsilon t; \qquad (38)$$

$$\Omega_0^2 = \omega_0^2 + \varepsilon \omega_1^2 + \ldots$$

Following the multiple scales method, after some transformations we derive the following equations:

$$\frac{\partial^2 \eta_0}{\partial T_0^2} + \omega_0^2 \eta_0 = 0; \eta_0 = A\,(T_1) \exp\left(\mathrm{i}\omega_0 T_0\right) + \bar{A}\,(T_1) \exp\left(-\mathrm{i}\omega_0 T_0\right); \qquad (39)$$

$$\frac{\partial^2 \eta_1}{\partial T_0^2} + \omega_0^2 \eta_1 + \omega_1^2 \eta_0 + 2\frac{\partial^2 \eta_0}{\partial T_0 \partial T_1} - h\eta_0 \sum_{s=1}^{\infty} \frac{s q_0^s}{(1-q_0^{2s})} \cos\left(\Omega_* s t\right) = 0. \qquad (40)$$

Resonances of order $s(s = 1, 2, 3 \ldots)$ are considered. The resonance conditions are presented as

$$\Omega_* s = 2\omega_0 + \varepsilon\sigma_s , \tag{41}$$

where σ_s is the detuning parameter. Using a change of variables: $A = \frac{a}{2}\exp(\mathrm{i}\beta)$; $\gamma = \sigma_s T_1 - 2\beta$, we can write the next system of modulation equations

$$\begin{aligned} a' w_0 &= a\chi \sin(\sigma_s T_1 - 2\beta) ; \\ \beta' \omega_0 &= \frac{\omega_1^2}{2} - \chi \cos(\sigma_s T_1 - 2\beta) , \end{aligned} \tag{42}$$

where $\chi = \dfrac{hsq_0^s}{4(1-q_0^{2s})}$. Equations (42) with respect to variables $(x, y) = [a\cos(\beta - 0.5\sigma_s T_1), a\sin(\beta - 0.5\sigma_s T_1)]$ are

$$\begin{aligned} x' &= y\left(\frac{\sigma}{2} - \frac{\omega_1^2}{2\omega_0} - \frac{\chi}{\omega_0}\right); \\ y' &= x\left(-\frac{\chi}{\omega_0} + \frac{\omega_1^2}{2\omega_0} - \frac{\sigma}{2}\right). \end{aligned} \tag{43}$$

The solutions of equations (37) have the form:

$$\eta = x\cos\left(\frac{\Omega_* s}{2}t\right) - y\sin\left(\frac{\Omega_* s}{2}t\right) + O(\varepsilon). \tag{44}$$

Now the stability analysis of the solutions of equation (37) is reduced to the system (43) analysis, i.e. a trivial solution stability is investigated. The eigenvalues of system (43) are

$$\lambda_{1,2} = \pm\sqrt{\frac{\chi^2}{\omega_0^2} - \left(\frac{\sigma}{2} - \frac{\omega_1^2}{2\omega_0}\right)^2}. \tag{45}$$

The following relation represents the boundary of the stable/unstable oscillations regions on the plane of the system parameters:

$$\Omega_* s = 2\omega_0 + \varepsilon\left(\frac{\omega_1^2}{\omega_0} \pm \frac{2\chi}{\omega_0}\right) + O(\varepsilon^2). \tag{46}$$

Using formulae (37) and (38), we can rewrite equations (46) to study the geometry of the stability/instability regions on parametric plane (c, W_*) as

$$\frac{\sqrt{2}cK(k_0)}{p\pi s} = \sqrt[4]{c^2(1-c)^2 + \frac{W_*^4}{4c^2} - (1-c)W_*^2 + O(\varepsilon)}. \tag{47}$$

Since the shallow snap-through truss is considered, the next notations are introduced: $1-c = \varepsilon_* c_1; \varepsilon_* \prec\prec 1$. Then, equation (47) has the following form

$$\frac{\sqrt{2}cK(k_0)}{p\pi s} = \frac{W_*}{\sqrt{2c}}\left(1-\varepsilon_*\frac{c^2c_1}{W_*^2}\right) + O\left(\varepsilon_*^2\right) + O(\varepsilon), \tag{48}$$

where

$$k_0^2 = \frac{1}{2} + \varepsilon_*\frac{c^2c_1}{W_*^2} + O\left(\varepsilon_*^2\right); \tag{49}$$

$$K(k_0) = K\left(\frac{1}{\sqrt{2}}\right) + \varepsilon_* K'\left(\frac{1}{\sqrt{2}}\right)\frac{c^2c_1}{\sqrt{2}W_*^2} + O\left(\varepsilon_*^2\right). \tag{50}$$

We can obtain from the equation (48):

$$W_* = \frac{2c^{3/2}}{p\pi s}\left[K\left(\frac{1}{\sqrt{2}}\right) + \varepsilon_*\frac{c^2c_1^2}{W_*^2}E\left(\frac{1}{\sqrt{2}}\right)\right] + O\left(\varepsilon_*^2\right) + O(\varepsilon). \tag{51}$$

Figure 7 shows curves (OA_1), (OA_2), (OA_3) on plane (c, W_*), which meet equation (51). Note that the terms of order $O(\varepsilon)$ are presented in formula (46). The boundaries of the stable/unstable regions are shown qualitatively in Figure 7 in the form of curves ($B_1C_1D_1$), ($B_2C_2D_2$), ($B_3C_3D_3$). Values $\tilde{c}_s; s = 1, 2, \ldots$, which are shown in Figure 7, are derived from equations (46) and (51). These values are determined according to the formula:

$$\tilde{c}_s = \left[1 + \frac{4K^2\left(\frac{1}{\sqrt{2}}\right)\left(\sqrt{2}-1\right)}{p^2\pi^2 s^2}\right]^{-1}. \tag{52}$$

Magnitudes $\tilde{c}_s$ have the following values: $\tilde{c}_1 = 0.63; \tilde{c}_2 = 0.88; \tilde{c}_3 = 0.94$ for the system parameters chosen in Section 3. In this case, points A_i $(i = 1, 2, 3)$ shown in Figure 7 have the following coordinates: A_1(1;1.18); A_2(1;0.59); A_3(1;0.39).

The following conclusions can be made from Figure 7. If φ is small, the unstable oscillations regions have order $O(\varepsilon)$. If the value of φ is increased, the width and number of the unstable regions are decreased. We can choose values of φ, such that the periodic motions under consideration are always stable.

4.2. Stability of the Periodic Motions with Small Amplitudes

Here we study the stability of the non-localized normal mode, which is considered in Section 3.1.2. Let us introduce variables $(\xi, \eta) = (u_2/g; -u_2/g + w_1)$. At configuration space (u_1, w_1) these variables coincide with the normal mode of linearized system (6). System (6) with respect to the above-mentioned variables has the following form

$$\ddot{\xi} + \xi + \varepsilon f_1(\xi, \eta) = 0; \tag{53}$$

$$\ddot{\eta} + 2s^2p^2\eta + \varepsilon f_2(\xi, \eta) = 0; \tag{54}$$

where

$$f_1(\xi, \eta) = \bar{\gamma}c^2\frac{p^2s^2-1}{2p^2s^2-1}\xi - \frac{\bar{\gamma}cs}{g}\eta;$$

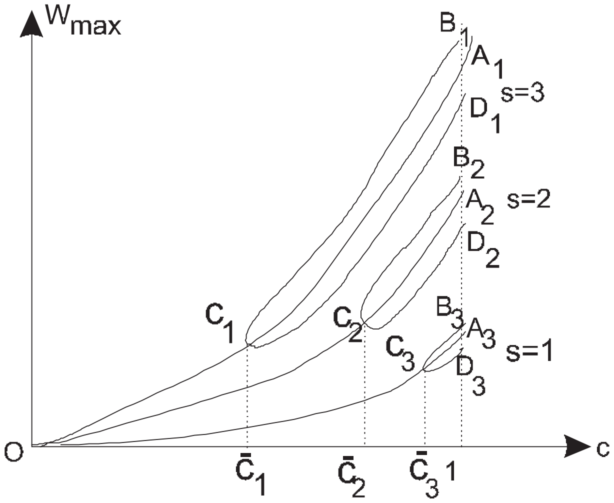

Figure 7. Stable/unstable regions on plane (c, W_*) for the NNM with large amplitudes. The boundaries of the regions are shown qualitatively in the form of curves ($B_1C_1D_1$), ($B_2C_2D_2$), ($B_3C_3D_3$). The curves (OA_1), (OA_2), (OA_3) meet equation (51).

$$f_2(\xi,\eta) = -\bar{\gamma}c^2\frac{p^2s^2-1}{2p^2s^2-1}\xi + \frac{\bar{\gamma}cs}{g}\eta + p^2\left(A\xi^2 + B\xi\eta + 3sc^2\eta^2\right);$$

$$A = 3sc^2 + \frac{1}{2}\tilde{\beta}g^2 + 2\tilde{\alpha}g; B = 6sc^2 + 2\tilde{\alpha}g.$$

We represent equation (53) solutions as

$$\xi = \xi_{\max}\cos(t) + O(\varepsilon), \tag{55}$$

where $\xi_{\max}$ is the oscillations amplitude. Relation (55) is substituted into equation (54). Small perturbations $\Delta\eta(t)$ determining the motion stability are added to the periodic motion $\eta(t)$. The variational equation to within the terms of order $O(\varepsilon)$ can be written in the form:

$$\Delta\ddot{\eta} + \left(2s^2p^2 + \varepsilon\frac{\bar{\gamma}cs}{g} + \varepsilon p^2B\xi_{\max}\cos(t)\right)\Delta\eta = 0. \tag{56}$$

The well-known asymptotic results on Mathieu's equation (Bogolubov and Mitropolski, 1961) are used, and the boundary of the stable/unstable regions in the system parameters space is obtained:

$$2\sqrt{2}ps^2 - 8p^2s^3 = \mp\varepsilon\xi_{\max}. \tag{57}$$

This boundary is shown in Figure 8, where $s = \sin\varphi$ is plotted on the x-axis. The periodic oscillations are unstable in the shaded region and they are stable outside this region. The point O with the coordinates $O(\sin\varphi_*, 0)$ is the cusp. Value φ_* is determined as

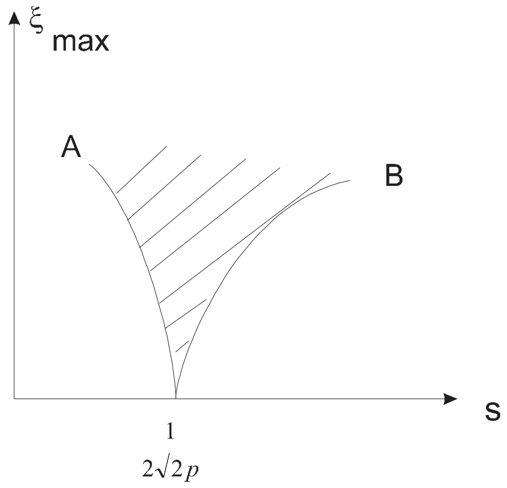

Figure 8. The stability/instability regions on system parameter plane $(\xi_{\max}, s)$ for the non-localized normal mode.

$$\varphi_* = \arcsin\left(\frac{1}{2\sqrt{2}p}\right).$$

For the numerical parameters used in Section 3.1, value φ_* is the next: $\varphi_* = 0.36$ radian. As follows from Figure 8 and formula (57), if amplitude $\xi_{\max}$ is increased, the stable periodic oscillations become unstable.

Now we study the stability of the periodic motions, which are determined in Section 3.1.1. Taking into account the following estimations for generalized coordinates, $w_1 = O(1)$; $u_1 = O(\varepsilon)$, we can present the second equation of system (6) in the form:

$$\bar{\mu}\ddot{w}_1 + 2\bar{\gamma}s^2 w_1 + O(\varepsilon) = 0. \tag{59}$$

The solution of equation (59) is

$$w_1 = W_*^{(\max)}\cos\left(ps\sqrt{2}t\right) + O(\varepsilon).$$

Then we consider the first equation of system (6):

$$\ddot{u} + \left(1 + \varepsilon\bar{\gamma}c^2 - \frac{\bar{\gamma}cs}{b_1}\right)u + \varepsilon^2\bar{\gamma}\left(\tilde{\beta}w_1 u + \tilde{\alpha}w_1^2\right) = 0. \tag{60}$$

Let us introduce small orthogonal variations $\Delta\eta(t)$ for the periodic motions. The equation with respect to $\Delta\eta$ can be written as

$$\Delta\ddot{\eta} + \left[2p^2s^2 + \varepsilon\bar{\gamma}c^2 + \varepsilon^2\bar{\gamma}\beta W_*^{(\max)}\cos\left(ps\sqrt{2}t\right)\right]\Delta\eta = 0. \tag{61}$$

This is the Mathieu equation, which is considered in various books (Bogolubov and Mitropolski, 1961). As a result, the following conclusions are made. There are no terms with resonance of order $O(\varepsilon^2)$. However, terms with resonance of order $O(\varepsilon^4)$ do arise. These terms are negligible. Therefore, the considered periodic motions are always stable to within order $O(\varepsilon^4)$.

5. CONCLUSIONS

In this paper we suggest the use of the snap-through truss to absorb oscillations. The main elastic system, of which oscillations are absorbed, is simulated by the linear 1-DOF oscillator. The free nonlinear oscillations of the 2-DOF system are analyzed by using the NNM method. The periodic motions stability is also considered.

On the basis of the above-expounded research, the following conclusion can be made. The localized NNM is the favorable regime to absorb oscillations. When the snap-through truss has significant amplitudes of oscillations, the main elastic system has small amplitudes. Note that the localized NNM is stable over a wide range of system parameters.

Acknowledgments. The authors especially thank Professor L. I. Manevich and Dr. O. Gendelman for many useful conversations on the topics presented in this paper. The work was supported in part by AFOSR Contract 00-AF-B/V-0813 (Dr. Dean Mook is the Grant Monitor).

REFERENCES

Alabuchev, P.M., Gritchin, A. A., and Kim, L. I., 1986, *Vibration Insulation Systems with Quasi-Zero Stiffness,* Mashinostroenie, Leningrad (in Russian).

Aoki, S. and Watanabe, T., 1994, "An investigation of an impact vibration absorber with hysteretic damping", in *Proceedings of the 2nd International Conference on Motion and Vibration Control,* Yokohama, Japan, pp. 468–474.

Bogolubov, N. N. and Mitropolski, Yu. A., 1961, *Asymptotic Methods in the Theory of Nonlinear Oscillations,* Gordon and Breach, NY.

Frolov, K. V., ed, 1995, *Vibrations in Engineering,* Mashinostroenie, Moscow (in Russian).

Haddow, A. G. and Shaw, S. W., 2001, "An experimental study of torsional vibration absorber," in *Proceedings of the ASME Design Engineering Technical Conference,* USA pp. 1–7.

Haxton, R. S. and Barr, A. D. S., 1972, "The autoparametric vibration absorber," *Journal of Engineering for Industry* **94**, 119–225.

Karyeaclis, M. P. and Caughey, T. K., 1989a, "Stability of a semi-active impact damper: Part I – Global behavior," *Transactions of the ASME, Journal of Applied Mechanics* **56**, 926–929.

Karyeaclis, M. P. and Caughey, T. K., 1989b, "Stability of a semi-active impact damper: Part II – Periodic solution," *Transactions of the ASME, Journal of Applied Mechanics* **56**, 930–940.

Lee, C.-T. and Shaw, S. W., 1995, "Torsional vibration reduction in internal combustion engines using centrifugal pendulums," in *Proceedings of the Design Engineering Technical Conference,* USA, Vol. 3, Part A, ASME, New York, pp. 487–492.

Manevitch, L. I., Mikhlin, Yu.V., and Pilipchuk, V. N., 1989, *Method of Normal Modes for Essentially Nonlinear Systems,* Nauka, Moscow (in Russian).

Natsiavas, S., 1992, "Steady state oscillations and stability of non-linear dynamic vibration absorber," *Journal of Sound and Vibration* **156(22)**, 227–245.

Natsiavas, S., 1993, "Vibration absorbers for a class of self-excited mechanical systems," *Transactions of the ASME, Journal of Applied Mechanics* **60**, 382–387.

Nayfeh, A. H., 1973, *Perturbation Methods,* Wiley, New York.

Shaw, S. and Shaw, S. W., 1989, "The onset of chaos in a two-degree-of-freedom impacting system," *Transactions of the ASME, Journal of Applied Mechanics* **56**, 168–174.

Shaw, S. W. and Wiggins, S., 1988, "Chaotic motions of a torsional vibration absorber," *Transactions of the ASME, Journal of Applied Mechanics* **55**, 952–958.

Shaw, J., Shaw, S. W., and Haddow, A. G., 1989, "On the response of the non-linear vibration absorber," *International Journal of Non-Linear Mechanics* **24(4)**, 281–293.

Vakakis, A. F., 2001, "An overview of motion localization and energy pumping in coupled nonlinear oscillators," in *Proceedings of the 6th Conference on Dynamical Systems Theory and Application,* Lodz, Poland, pp. 111–118.

Vakakis, A. F., Manevitch, L. I., Mikhlin, Yu. V., Pilipchuk, V. N., and Zevin, A. A., 1996, *Normal Modes and Localization in Nonlinear Systems,* Wiley Interscience, NY.